Incorporating free-surface multiples in Marchenko imaging

S. Singh[1], R. Snieder[1], J. van der Neut[2], J. Thorbecke[2], E. Slob[2], K. Wapenaar[2]
(1) Center for Wave Phenomena, Department of Geophysics, Colorado School of Mines, Golden, Colorado, USA
(2) Department of Geoscience and Engineering, Delft University of Technology, GA Delft, The Netherlands

SUMMARY

Imagine placing a receiver at any location in the Earth and recording the response at that location to sources on the surface. In such a world, we could place receivers around our reservoir to better image the reservoir and understand its properties. Realistically, this is not a feasible approach for understanding the subsurface. Here, we present an alternative and realizable approach to obtaining the response of a buried virtual receiver for sources at the surface. This method is capable of retrieving the Green's function for a virtual point in the subsurface to the acquisition surface. In our case, a physical receiver is not required at the subsurface point; instead, we require the reflection measurements for sources and receivers at the surface of the Earth and a macro-model (no small-scale details of the model are necessary). We can interpret the retrieved Green's function as the response to sources at the surface for a virtual receiver in the subsurface. We obtain this Green's function by solving the Marchenko equation, an integral equation pertinent to inverse scattering problems. Our derivation of the Marchenko equation for the Green's function retrieval takes into account the free-surface reflections. We decompose the Marchenko equation into up- and down-going fields and solve for these fields iteratively. We use these up- and down-going fields, which includes the free-surface multiples, to obtain a 2D image of our area of interest, in this case, below a synclinal structure. This imaging is called Marchenko imaging.

INTRODUCTION

Traditionally, to image the subsurface using standard imaging methods like reverse time migration (RTM) or Kirchhoff migration, one assumes the first-order Born approximation. This assumption only allows us to use primary reflections in conventional imaging (single-scattered waves). However, the assumption of the first Born approximation leads to artifacts in the presence of multiples. In order to implement conventional imaging and to ensure the assumption of single scattering holds, one has to remove multiply reflected waves. Multiples consist of internal and free-surface multiples. The removal of free-surface multiples is generally a priority in the recorded reflection response since free surface multiples are, in general, stronger than internal multiples. Removing the multiples is not always a simple task; in addition, removal does not allow us to use the valuable information provided by these multiples. Multiples provide redundant as well as new information that is still useful to improve our image. Using multiples can increase the illumination and lead to better vertical resolution in the image (Schuster et al., 2003; Jiang et al., 2007; Muijs et al., 2007a,b).

We propose to use an inverse scattering approach for imaging multiples. The physical basis for exact inverse scattering is focusing and time reversal (Rose, 2002b,a), which yield the Marchenko equation. This equation is an integral equation that determines the wavefield for a (virtual) source at any point $\mathbf{x}$, i.e., the retrieved Green's function, given the impulse response function. Broggini et al. (2012) extend the work of Rose (2002a) to geophysics for retrieving the Green's function from reflected waves at the surface. These Green's functions from the retrieval include only primaries and internal multiples (Broggini et al., 2012, 2014). They use the Green's function to image the subsurface (Marchenko imaging), whereby they minimize the artifacts produced by internal multiples. Marchenko imaging uses the up- and down-going Green's function for imaging. We have incorporated the free-surface multiples in the retrieval of the Green's function algorithm (Singh et al., 2015); therefore our retrieved Green's functions also include free-surface multiples with the internal multiples and primaries. The major differences between our previous work (Singh et al., 2015) and this work are: (1) we use pressure-normalized wavefields compared to flux-normalized wavefields to obtain the Marchenko-type equations, and (2) we show 2D imaging examples.

There is another approach to imaging using inverse scattering proposed by Weglein et al. (2003), who uses a non-closed or series solution called the inverse scattering series. Unlike in the work of Weglein et al. (2003), our inverse solution to the wave equation is in the form of Fredholm integral equations of the second kind (Marchenko-type equations).

In this paper, we derive the retrieval of the Green's function by solving Marchenko-type equations using pressure-normalized wavefields. For more details on pressure versus flux-normalized wavefields see Wapenaar and Grimbergen (1996) and Wapenaar (1998). We show numerical examples of imaging the subsurface using the Green's functions at different depths. Note that the Green's function includes primaries, internal multiples, and free-surface multiples, so we are using all the scattered events in the imaging. We call imaging with these Green's functions Marchenko imaging. The distinction with our work and the previous papers Wapenaar et al. (2014a), Slob et al. (2014) and Wapenaar et al. (2014b) is that we include free-surface multiples in the imaging.

THEORY

Retrieving the Green's function in the presence of a free surface, using Marchenko-type equations, is derived in multi-dimensions by Singh et al. (2015), but their numerical examples are one dimensional. The reflection response R that Singh et al. (2015) uses to retrieve these functions is flux-normalized, which fa-

cilitates the derivation of the 3D Marchenko equations (Wapenaar et al., 2014a). Similarly, the retrieval of the Green's function without a free surface also uses flux-normalized wavefields, (Broggini et al., 2012; Wapenaar et al., 2013). However, the Green's function retrieval is not restricted to flux-normalized fields and can be modified to pressure-normalized fields. Wapenaar et al. (2014a) derive the retrieval of the Green's function using pressure-normalized fields in the absence of a free surface. In this paper, we demonstrate an alternative approach by using pressure-normalized fields to retrieve the Green's function in the presence of a free surface.

We begin the retrieval of the Green's function derivation with the frequency-domain one-way reciprocity theorems of the convolution and correlation type (Wapenaar et al., 2014a), which hold for lossless media between ∂D_0 (acquisition surface) and ∂D_i (arbitrary depth level):

$$\begin{aligned}\int_{\partial D_0} \rho^{-1}(\mathbf{x})[(\partial_3 p_A^+)p_B^- + (\partial_3 p_A^-)p_B^+]d\mathbf{x_0} = \\ -\int_{\partial D_i} \rho^{-1}(\mathbf{x})[p_A^+(\partial_3 p_B^-) + p_A^-(\partial_3 p_B^+]d\mathbf{x_i},\end{aligned} \tag{1}$$

$$\begin{aligned}\int_{\partial D_0} \rho^{-1}(\mathbf{x})[(\partial_3 p_A^+)^* p_B^+ + (\partial_3 p_A^-)^* p_B^-]d\mathbf{x_0} = \\ -\int_{\partial D_i} \rho^{-1}(\mathbf{x})[(p_A^+)^*(\partial_3 p_B^+) + (p_A^-)^*(\partial_3 p_B^-)]d\mathbf{x_i}.\end{aligned} \tag{2}$$

The asterisk * denotes complex conjugation, and the subscripts A ans B are two wave states. Equations 1 and 2 are the reciprocity theorems for pressure-normalized one-way wavefields. Equation 2 does not account for evanescent waves. The spatial coordinates are defined by their horizontal and depth components, for instance $\mathbf{x_0} = (\mathbf{x_H}, x_{3,0})$, where $\mathbf{x_{H,0}}$ are the horizontal coordinates at a depth $x_{3,0}$. These one-way reciprocity theorems hold for up- and down-going pressure-normalized fields.

One-way wavefields

The reciprocity theorems are used to solve for the Green's function. We define the Green's function as the response to an impulsive point source at $\mathbf{x_0''}$ just above ∂D_0 of volume injection rate. This Green's function obeys the scalar wave equation

$$\rho \bigtriangledown \cdot \left(\frac{1}{\rho} \bigtriangledown G\right) - \frac{1}{c^2}\frac{\partial^2 G}{\partial t^2} = -\rho\delta(\mathbf{x}-\mathbf{x_0''})\frac{\partial \delta(t)}{\partial t}. \tag{3}$$

We include the time derivative on the right hand side because we consider the source to be of volume injection rate. Since we are using one-way reciprocity theorems, equations 1 and 2, we define our Green's function (two-way) as a sum of the up- and down-going pressure-normalized one-way Green's functions, which in the frequency domain is given by

$$G(\mathbf{x}, \mathbf{x_0''}, \omega) = G^{+,q}(\mathbf{x}, \mathbf{x_0''}, \omega) + G^{-,q}(\mathbf{x}, \mathbf{x_0''}, \omega), \tag{4}$$

where $\mathbf{x}$ is the observation point. Defined this way, the one-way Green's functions are decomposed at the observation point $\mathbf{x}$ denoted by the first superscript $+$ or $-$. We consider downwards to be positive, hence the superscript $+$ represents down-going waves and $-$ up-going waves. The second superscript (q) refers to the volume-rate injection source at $\mathbf{x_0''}$. For instance, $G^{-,q}(\mathbf{x}, \mathbf{x_0''}, \omega)$ is the pressure-normalized up-going Green's function at $\mathbf{x}$ due to a volume injection source at $\mathbf{x_0''}$ in the frequency domain.

On ∂D_0:	p_B^+	$= f_1^+(\mathbf{x_0}, \mathbf{x_i'}, \omega)$,	
	p_B^-	$= f_1^-(\mathbf{x_0}, \mathbf{x_i'}, \omega)$.	
On ∂D_i:	$\partial_3 p_B^+$	$= \partial_3 f_1^+(\mathbf{x_i}, \mathbf{x_i'}, \omega)$	$= -\frac{1}{2} j\omega\rho(\mathbf{x_i'})\delta(\mathbf{x}_H - \mathbf{x_H'})$,
	$\partial_3 p_B^-$	$= \partial_3 f_1^-(\mathbf{x_i}, \mathbf{x_i'}, \omega)$	$= 0$.

Table 1: The one-way wavefields of the focusing function f_1 at the acquisition surface ∂D_0 and the level where f_1 focuses, ∂D_i. $p_B^{\pm}$ symbolizes one-way wavefields in the frequency domain, at arbitrary depth levels in the reference medium.

Similar to equation A11 in Wapenaar et al. (2014a), we define the vertical derivative of the up-going Green's function at the acquisition surface ∂D_0 as

$$\partial_3 G^{-,q}(\mathbf{x}, \mathbf{x_0''}, \omega)|_{x_3=x_{3,0}} = \frac{1}{2} j\omega\rho(\mathbf{x_0})R(\mathbf{x_0''}, \mathbf{x_0}, \omega).$$

However in our case, both $\partial_3 G^{-,q}$ and R include the free-surface multiples. Considering the downward component of the source and the surface-reflected waves, we define

$$\begin{aligned}&\partial_3 G^{+,q}(\mathbf{x}, \mathbf{x_0''}, \omega)|_{x_3=x_{3,0}} = \\ &-\frac{1}{2}\left(j\omega\rho(\mathbf{x_0})\delta(\mathbf{x_H} - \mathbf{x_H''}) + j\omega\rho(\mathbf{x_0})\mathbf{r}R(\mathbf{x_0''}, \mathbf{x_0}, \omega)\right),\end{aligned}$$

where $\mathbf{r}$ denotes the reflection coefficient of the free surface. For the down-going field $\partial_3 G^{+,q}$, at and below ∂D_0, we consider both the downward component of the source $-\frac{1}{2} j\omega\rho(\mathbf{x_0})\delta(\mathbf{x_H} - \mathbf{x_H''})$ and the reflections from the free surface $-\frac{1}{2} j\omega\rho(\mathbf{x_0})\mathbf{r}R(\mathbf{x_0''}, \mathbf{x_0}, \omega)$, similar to the Marchenko derivation with flux-normalized fields from Singh et al. (2015). At ∂D_i, the up- and down-going waves are $G^{-,q}$ and $G^{+,q}$, respectively. These one-way wavefields in the actual medium are defined as State A.

Similar to previous papers that derive Marchenko-type equations (Wapenaar et al., 2013, 2014a; Slob et al., 2014; Singh et al., 2015), we also define focusing functions. The focusing function f_1 is a solution for the waves that focus at a point just below the bottom of the truncated medium. The truncated medium is called the reference medium as it is reflection free above and below ∂D_0 and ∂D_i, respectively, but is the same as the actual medium between ∂D_0 and ∂D_i. The f_1 function is defined as waves that focus at $\mathbf{x_i'}$ at a defined depth level (∂D_i) for incoming f_1^+ and outgoing f_1^- waves at the acquisition surface (∂D_0) $\mathbf{x_0}$.

The one-way wavefields for the f_1 function at the depth levels ∂D_0 and ∂D_i are defined as State B. The one-way focusing function $f_1^+(\mathbf{x}, \mathbf{x_i'}, t)$ is shaped such that $f_1(\mathbf{x}, \mathbf{x_i'}, t)$ focuses at $\mathbf{x_i'}$ at $t = 0$. At depth level of the focusing point $\mathbf{x_i'}$ of f_1, we define $\partial_3 f_1(\mathbf{x}, \mathbf{x_i'}, t)$ as $\frac{1}{2}\rho(\mathbf{x_i'})\delta(\mathbf{x}_H - \mathbf{x_H'})\partial\delta(t)/\partial t$, a two-dimensional (2D) and 1D Dirac delta function in space and time, respectively (see Table 1). After the focusing point, $f_1(\mathbf{x}, \mathbf{x_i'}, t)$ continues to diverge as a down-going field $f_1^+(\mathbf{x}, \mathbf{x_i'}, t)$

into the reflection-free reference half-space (Wapenaar et al., 2014a).

By substituting the one-way wavefields given in the actual (State A) and reference (State B) medium into the convolution reciprocity theorem, 1, we get the up-going Green's function

$$G^{-,q}(\mathbf{x_i'},\mathbf{x_0''},\omega) = -f_1^-(\mathbf{x_0''},\mathbf{x_i'},\omega) + \int_{\partial D_0}[f_1^+(\mathbf{x_0},\mathbf{x_i'},\omega)R(\mathbf{x_0''},\mathbf{x_0},\omega) - \mathbf{r}f_1^-(\mathbf{x_0},\mathbf{x_i'},\omega)R(\mathbf{x_0''},\mathbf{x_0},\omega)]d\mathbf{x_0}. \quad (5)$$

Likewise, substituting the one-way wavefields in the actual (State A) and reference (State B) medium into the correlation reciprocity theorem, 2, we get the down-going Green's function

$$G^{+,q}(\mathbf{x_i'},\mathbf{x_0''},\omega) = f_1^+(\mathbf{x_0''},\mathbf{x_i'},\omega)^* - \int_{\partial D_0}[f_1^-(\mathbf{x_0},\mathbf{x_i'},\omega)^*R(\mathbf{x_0''},\mathbf{x_0},\omega) - \mathbf{r}f_1^+(\mathbf{x_0},\mathbf{x_i'},\omega)^*R(\mathbf{x_0''},\mathbf{x_0},\omega)]d\mathbf{x_0}. \quad (6)$$

Equations 5 and 6 are identical to the equations for G^- and G^+ of Singh et al. (2015), however our Green's functions are pressure normalized. Hence, we can directly solve for the one-way Green's functions in equations 5 and 6 with an iterative scheme similar to Singh et al. (2015). The equations that we use to obtain the focusing function are called the Marchenko equations.

Marchenko imaging

Broggini et al. (2012, 2014); Wapenaar et al. (2011); Slob et al. (2014); Wapenaar et al. (2014b); Singh et al. (2015) have all used the one-way retrieved Green's functions to produce an image. Marchenko imaging is built on the concept of obtaining the redatumed reflection response from the up- and down-going wavefields at an arbitrary depth level. The use of up- and down-going wavefield for imaging is not a new principle. Claerbout (1971), Wapenaar et al. (2000) and Amundsen (2001) have shown that one can get the reflection response below an arbitrary depth level once the up- and down-going wavefields are available at that depth level.

The governing equation for imaging with such one-way wavefields is, in the time domain, (Wapenaar et al., 2008)

$$G^{-,q}(\mathbf{x_i'},\mathbf{x_0''},t) = \int_{\partial D_i} d\mathbf{x_i}\int_{-\infty}^{\infty} G^{+,q}(\mathbf{x_i},\mathbf{x_0''},t-t')R_0(\mathbf{x_i'},\mathbf{x_i},t')dt', \quad (7)$$

where ∂D_i is an arbitrary depth level and R_0 is the reflection response of the medium below ∂D_i. Note that equation 7 holds for out- and in-going wavefields normal to the surface ∂D_i. However, Green's function retrieval (current methods) retrieves strictly up- and down-going wavefields at arbitrary depth levels, which corresponds to a flat surface ∂D_i. The reflection response R_0, in equation 7, is the response as if everything above ∂D_i is transparent. Therefore, R_0 is a virtual reflection response as if there were receivers and sources at ∂D_i, in the absence of a free-surface at ∂D_i. Significantly, the response R_0 is blind to the overburden above ∂D_i. Wapenaar et al. (2014b) have shown the retrieval of this virtual reflection below a complex overburden. In this paper, any variable with a subscript 0 (e.g., R_0) indicates that no free-surface is present.

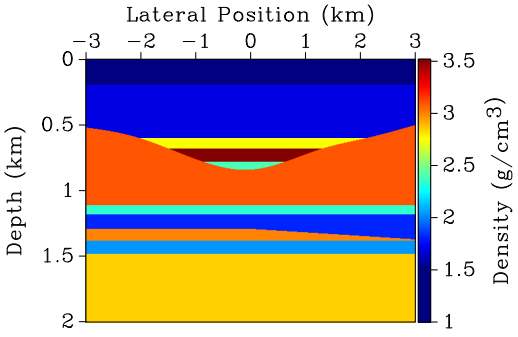

Figure 1: The density model ranging from densities 1 to 3.5 g/cm^3 as shown in the color bar.

We choose to solve for R_0 in equation 7 by multidimensional deconvolution (MDD) (van der Neut et al., 2011). Details of solving equation 7 using retrieved Green's functions are given in Wapenaar et al. (2014b). The significant difference between our work and the previous Marchenko imaging papers is that our Green's functions include information of the actual medium with the free-surface and includes all (free-surface and internal) multiples. This corresponds to using the free-surface multiples in the imaging. Once we obtain R_0 at each image point, our subsurface image is the contribution of R_0 at zero offset and zero time, i.e., $R_0(\mathbf{x_i},\mathbf{x_i},0)$.

NUMERICAL EXAMPLES

Our numerical model has a constant velocity of 2.5 km/s with variable density, as shown in Figure 1, however, constant velocity is not a restriction of our algorithm. The density is a 2D inhomogeneous subsurface model with a syncline structure. The horizontal range of the model is -3000 m to 3000 m. Our goal is to show: (1) the retrieval of the Green's function $G(\mathbf{x_i'},\mathbf{x_0''},t)$ for a virtual receiver at $\mathbf{x_i'} = (0,1100)$ m and the corresponding variable source locations at $\mathbf{x_0''}$ and (2) the subsurface image below the syncline structure. To obtain the Green's function, we need the pressure-normalized reflection response $R(\mathbf{x_0''},\mathbf{x_0},\omega)$ and a macro-model (no small-scale details of the model are necessary. The reflection response is computed by finite differences Thorbecke and Draganov (2011) with vertical-force sources and particle-velocity receiver recordings, both at the surface. The receiver spacing is 10 m and the source is a Ricker wavelet with a central frequency of 20 Hz. We use this finite-difference response reflection response, which we deconvolve with the source wavelet, and decompose it into the up-going pressure $R(\mathbf{x_0''},\mathbf{x_0},\omega)$. The macro-model is a smooth version of the velocity model, in this case we just need the constant velocity model. No information of the density is required. In the situation where the velocity model is varying, the macro-model will be a smooth version of the velocity model, since we only need the macro-model to compute the travel times of the direct arrival.

Green's function retrieval

Equations 5 and 6 are evaluated for $t < t_d$ to resolve the focusing functions iteratively from R (where t_d is the first-arrival

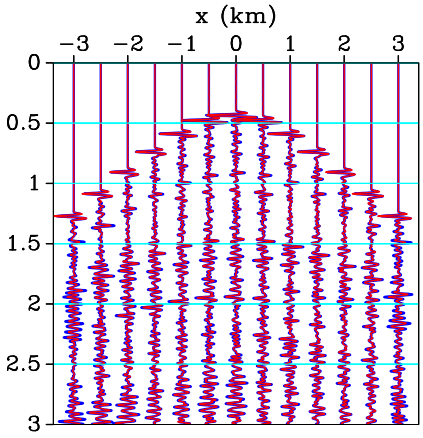

Figure 2: The retrieved two-way Green's function [in red] superimposed on the modeled Green's function (computed by finite differences with the small-scale details in the density model included)[in blue].

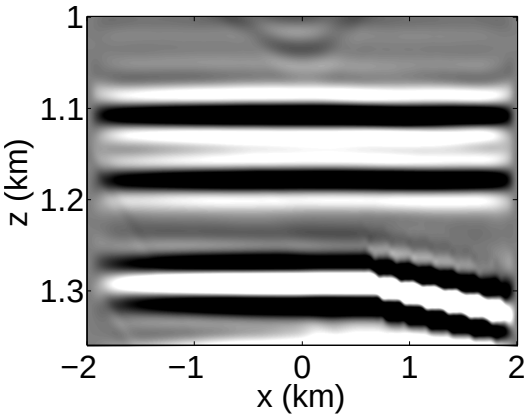

Figure 3: Target-oriented Marchenko imaging of the model in Figure 1 below the syncline structure. The image is $R_0(\mathbf{x_i},\mathbf{x_i},0)$ for $\mathbf{x_i}$ ranging from $\mathbf{x_{H,i}} = -2$ to 2 *km* and $x_{3,i} = 1$ to 1.36 *km*.

time of the Green's function). By substituting the focusing functions in equations 5 and 6 we obtain the one-way pressure-normalized Green's functions. The two-way Green's function is given as the summation of the up- and down-going Green's function. A comparison of this retrieved two-way Green's function to the modeled Green's function (modeled with the exact small-scale variations in the density) is shown in Figure 2. For display, we apply a gain of $\exp(1.5*t(s))$ to the Green's functions in Figure 2 to better see the internal multiples and free-surface multiples at depth. The retrieved and modeled Green's function match almost perfectly, as shown in Figure 2. As expected, the far-offsets do not provide a good match of the amplitude because we are truncating the spatial integrals in the Marchenko equations.

Marchenko imaging -Target oriented

Target-oriented Marchenko imaging entails retrieving the up- and down-going Green's functions in the target area and using them to construct the image. Figure 3 shows the Marchenko image of the model in Figure 1. To compute this image we retrieve the up- and down-going Green's function $G^{\pm,q}(\mathbf{x}'_\mathbf{i},\mathbf{x}''_\mathbf{0},t)$ at the virtual receiver locations $\mathbf{x}'_\mathbf{i} = (\mathbf{x_H},x_{3,i})$ ranging from $\mathbf{x_{H,i}} = -2$ to 2 *km* and $x_{3,i} = 1$ to 1.36 *km*. We sampled $\mathbf{x_{H,i}}$ and $x_{3,i}$ every 0.040 *km* and 0.05 *km*, respectively, to retrieve the Green's function. These functions are used to compute $R_0(\mathbf{x_i},\mathbf{x}'_\mathbf{i},t)$ as explained in the theory section. The contribution to the image is $R_0(\mathbf{x_i},\mathbf{x_i},0)$, which is R_0 at zero-offset and zero time for the range of $\mathbf{x_i}$.

The target-oriented Marchenko image, Figure 3, is free of artifacts caused by the internal multiples and free-surface multiples in the overburden. This is because Marchenko imaging correctly migrates the primaries and all multiples to the correct reflector location. If the free-surface multiples were not handled correctly by Marchenko imaging then the associated multiples caused by the syncline and the layers within the syncline would be present in our image. This is because Marchenko imaging correctly migrates the primaries and all multiples to the correct reflector location.

CONCLUSION

We have shown that we can retrieve the Green's function at any location in the model without any knowledge of the small-scale variations of the subsurface once we have sufficient aperture coverage on the surface over the virtual source location. To retrieve the Green's function, we require the reflection response at the surface and a macro-model of the subsurface overburden (at least between the surface and the virtual source depth level). The major distinction between our work and the previous work on Marchenko imaging is that we include free-surface multiples in the Green's function retrieval, and hence also use these multiples in imaging.

In the numerical examples, we observe no significant artifacts in the Marchenko image, due to misplaced multiples, even though the reflection response includes multiples (no preprocessing is done to remove the multiples). How the multiples improve the image is yet to be investigated; however, for certain, Marchenko imaging naturally migrates the multiples (and primaries) to the correct reflector location. Significantly, the inputs for Marchenko imaging and for the current state-of-the-art imaging techniques are the same: the reflection response and a macro-model. However, in Marchenko imaging, we accurately handle not only the primaries but also the multiples.

ACKNOWLEDGMENTS

This work was funded by the sponsor companies of the Consortium Project on Seismic Inverse Methods for Complex Structures. The numeric examples in this paper are generated with the Madagascar open-source software package freely available from http://www.ahay.org.